Local Structure and Vibrational Properties of α'-Pu Martensite in Ga-stabilized δ-Pu

E. J. Nelson[1], K. J. M. Blobaum[2], M. A. Wall[2], P. G. Allen[1], A. J. Schwartz[2], C. H. Booth[3]

[1] *Seaborg Institute for Transactinium Science, Lawrence Livermore National Laboratory, P.O. Box 808, Livermore, CA 94551*

[2] *Materials Science and Technology Division, Lawrence Livermore National Laboratory, P.O. Box 808, Livermore, CA 94551*

[3] *Chemical Sciences Division, Lawrence Berkeley National Laboratory, Berkeley, CA 94720*

PACS numbers: 61.10.Ht, 61.66.Dk, 63.20.Dj, 81.30.Kf

ABSTRACT

Extended x-ray absorption fine structure spectroscopy (EXAFS) is used to investigate the local atomic environment and vibrational properties of plutonium and gallium atoms in the α' and δ phases of a mixed phase Pu-Ga alloy. EXAFS results measured at low temperature compare the structure of the mixed phase sample with a single-phase δ-Pu sample. EXAFS spectral components attributed to both α'-Pu and δ-Pu were observed in the mixed phase sample. Ga K-edge EXAFS spectra indicate local atomic environments similar to the Pu L_{III}-edge EXAFS results, which suggests that Ga is substitutional for Pu atoms in both the monoclinic α'-Pu and the fcc δ-Pu structures. In δ-Pu, we measure a Ga-Pu bond length contraction of 0.11 Å with respect to the Pu-Pu bond length. The

corresponding bond-length contraction around Ga in δ'-Pu is only 0.03 Å. Results from temperature-dependent Pu L_{III}-edge EXAFS measurements are fit to a correlated Debye model, and a large difference in the Pu-Pu bond Debye temperature is observed for the δ' and δ phases: $\Theta_D(\delta') = 159 \pm 13$ K versus $\Theta_D(\delta) = 120 \pm 3$ K. The corresponding analysis for the Ga K EXAFS determines a Ga-Pu bond Debye temperature of $\Theta_D(\delta) = 188 \pm 12$ K in the δ-Pu phase. These results are related to the observed solubility of Ga in δ-Pu, the "stabilization" of δ-Pu by Ga at room temperature, and the insolubility of Ga in δ'-Pu.

I. INTRODUCTION

Plutonium can exhibit at least six different solid phases, depending upon the temperature and alloying characteristics.[1] The face-centered cubic δ phase is stable from T = 593 K to 736 K in pure Pu. At room temperature and below, pure Pu exists in the monoclinic α phase, which has a complex structure with sixteen atoms in the unit cell. Small additions of Ga can "stabilize" the δ phase in Pu down to room temperature.[2] Upon further cooling of Ga-doped Pu, a diffusionless martensitic transformation of the alloy occurs for Ga concentrations below 3.3 at%. However, the transformation does not go all the way to completion, resulting in a mixed phase alloy.[3] In the transformed regions, the δ structure, in which Ga atoms are soluble, changes to the δ' structure, in which Ga atoms are insoluble but effectively trapped due to the very slow diffusion rates of Ga in the α matrix.[2] This metastable δ' phase consists of Ga dopant atoms trapped within a monoclinic α-Pu matrix.

The transition from the δ to the α' phase results in a 25% volume contraction. This large effect is believed to be due to a change in the nature of the Pu 5f electrons from delocalized (δ') to localized (δ). Pu marks the transition in the electronic character of the actinides from the delocalized behavior of the light actinides (Ac-Np) to the localized, lanthanide-like behavior of the heavier actinides.[4, 5] Because of the large differences in the mechanical and electronic properties of the two phases, this complex δ –> α' martensitic phase transformation in Pu-Ga alloys has been the subject of many experimental and theoretical studies.[2-3, 6-10] The role of Ga in the transformation, its "stabilization" of the δ-Pu phase at room temperature, and its location in the resulting mixed δ-Pu / α'-Pu material are several important issues which still need to be resolved in the understanding of this system, and which are addressed by the results of this study.

Here, we use a combined approach of optical microscopy and extended x-ray absorption fine structure spectroscopy (EXAFS) to investigate the phase morphology and local atomic environment of plutonium and gallium atoms for a reference Pu/Ga alloy before and after the δ –> α' martensitic partial transformation. The element-specific nature of EXAFS and its lack of a requirement for long-range order in the sample make it a suitable probe of the local structure surrounding the Ga and Pu atoms in a mixed δ-Pu / α'-Pu matrix. Specific signatures of δ-Pu and α'-Pu are observed in the Pu L_{III}- and Ga K-edge EXAFS of the partially transformed alloy. The Ga-Pu nearest-neighbor bond lengths are determined in each of the phases and compared to the corresponding Pu-Pu bond lengths. By examining the thermal dependence of the Debye-Waller factor of each phase component in the EXAFS data of the mixed phase alloy, pair-specific (Ga-Pu or Pu-Pu) Debye temperatures Θ_D are determined in both the δ-Pu and α'-Pu phases. A

comparison of the Debye temperatures of Ga-Pu and Pu-Pu bonds in each of the phases is related to the observed difference between the solubility of Ga in δ-Pu and the insolubility of Ga in α'-Pu, and to the "stabilization" of the δ-Pu phase by alloying with Ga.

The outline of the paper is as follows. Details of sample preparation and EXAFS experimental setup and data analysis are discussed in Sec. II. The results of curve-fitting analysis and fitting the temperature dependence of the EXAFS Debye-Waller factors to the correlated Debye model are presented in Sec. III. A discussion of the results in the context of the local atomic structure and the vibrational properties of bonding in the α' and δ phases is presented in Sec. IV, and the conclusions are given in Sec. V.

II. EXPERIMENTAL DETAILS

A. Sample preparation

All sample preparations were done at Lawrence Livermore National Laboratory (LLNL) using bulk δ-Pu from a sample batch of two-year-old ^{239}Pu alloy of known ~1.9 at. % Ga content. One bulk specimen of this reference alloy was maintained in the δ-Pu phase as a control, while another specimen was quenched to 148 K (-125ºC) and held at that temperature for 9 hrs. This temperature corresponds to the “nose” of the temperature-time-transformation curve for ~1.9 at. % Ga-doped δ-Pu alloy.[3] For this Ga concentration, the selected temperature was the one at which the δ-Pu –> α'-Pu martensitic transformation is expected to proceed most rapidly. Figure 1 shows optical

micrographs of the untransformed and partially transformed bulk samples. The untransformed sample contains the fcc δ-Pu phase with no significant amounts of other Pu phases present. In the partially transformed sample, the long, thin martensitic platelets are characteristic of the δ'-Pu phase, while the uniform matrix is δ-Pu. Based on the micrographs, the partially transformed sample contains 25 ± 5% δ'-Pu and 75 ± 5% δ-Pu by volume. Given the 25% volume difference between equal masses of the two phases, this corresponds to 29 ± 5% δ'-Pu and 71 ± 5% δ-Pu by mass. In order to achieve the preferred thickness for EXAFS transmission measurements, the two bulk pieces were reduced in thickness to ~14 μm in a series of sawing, lapping, and mechanical polishing steps. In the last step, the foils were electropolished down to the final thickness of 8-10 μm, which also removed any accumulated oxide material on the surface. All of these sample preparation steps were performed in an inert nitrogen atmosphere glove box. The sample was then encapsulated under nitrogen using a specially designed, triple containment x-ray compatible cell, as described elsewhere.[11] The triple-contained sample was subsequently mounted in an open cycle liquid helium flow cryostat for variable temperature EXAFS measurements. Temperature measurement errors are within ~1 K, and are stable within ~0.2 K. EXAFS measurements began 22 days after the partial δ –> δ' phase transformation was induced by the quench and isothermal hold.

B. EXAFS data acquisition and analysis

Plutonium L_{III} - and gallium K-edge x-ray absorption spectra were collected at the Stanford Synchrotron Radiation Laboratory (SSRL) on wiggler side station beamline 4-1 under normal ring operating conditions using a Si (220), half-tuned, double-crystal

monochromator operating in unfocussed mode. The vertical slit height inside the x-ray hutch was 0.9 mm, which reduces the effects of beam instabilities and monochromator glitches while providing ample photon flux. The horizontal slits were set at a width of 1.8 mm, which is smaller than the diameter of the sample (2.8 mm). The Pu L_{III} -edge spectra were measured in transmission mode using Ar-filled ionization chambers. The Ga K-edge spectra were measured in fluorescence mode using a 4-element Ge array solid-state detector developed at Lawrence Berkeley National Laboratory.[12] The detector was operated at ~25 kHz per channel and the Ga Kα fluorescence line was selected with single channel analyzer electronics.

XAFS raw data treatment, including calibration, normalization, and subsequent processing of the EXAFS and XANES (x-ray absorption near-edge structure) spectral regions was performed by standard methods reviewed elsewhere[13, 14] using the EXAFSPAK suite of programs developed by G. George of SSRL. Typically, two Pu transmission and four Ga fluorescence XAFS scans were collected from each sample at each temperature and the results were averaged. The Pu L_{III} -edge spectra were energy calibrated by simultaneously measuring the absorption spectrum for the reference powder PuO_2, while the Ga K-edge spectra were self-calibrated, due to the opacity of the sample at ~10 keV photon energy. The energies of the first inflection points for the reference sample absorption edges, E_r, were defined at 18053.1 eV (Pu L_{III}) and 10368.2 eV (Ga K). The EXAFS amplitudes were normalized relative to the smoothly varying absorption background $\mu_0(E)$. The background optimization code AUTOBK[15] was used to fit $\mu_0(E)$ using a piecewise spline that minimizes the spectral weight of the EXAFS real-space Fourier transform (FT) below R < 1.9 Å.

Nonlinear least squares curve fitting was performed on the k^3-weighted data using the EXAFSPAK program OPT. The EXAFS data were fit using theoretical phase and amplitude functions calculated from the program FEFF8.1 developed by Rehr *et al.*[16, 17] All of the Pu-Pu interactions were modeled using single scattering (SS) paths whose lengths were derived from the Pu model structures determined from x-ray diffraction, namely unalloyed fcc δ-Pu, a_{fcc} = 4.6371 Å,[18] and unalloyed monoclinic α-Pu, a = 6.183 Å, b = 4.822 Å, c = 10.963 Å, β = 101.79°.[19] The Ga-Pu SS interactions were modeled by using the same Pu model structures and replacing the central absorbing atom with Ga.

The EXAFS data were smoothed with a Gaussian peak of width Δk = 0.12 eV in order to reduce the experimental noise for better fitting. The amplitude reduction factor S_0^2 was fixed at a value of 0.55 for Pu and 0.85 for Ga, as determined from our previous EXAFS measurement of a 3.3 at% Ga-doped δ-Pu sample.[11] The energy shift ΔE_0 was first varied for each of the spectra in the data set, and then fixed at the average over all of the data set for the final fit to determine the Debye-Waller factors (+6.2 eV for Ga, –20.0 eV for Pu). The k-ranges used for all but the highest temperatures were [2.8 $Å^{-1}$, 12.5 $Å^{-1}$] for Pu and [2.6 $Å^{-1}$, 12.45 $Å^{-1}$] for Ga. At higher temperatures ($T \geq 200$ K) the higher end of the k-range was truncated to ~ 11 Å, since thermal effects damp out the EXAFS signal at higher k values. The EXAFS is weighted by a factor of k^3 for the fits and for plotting the data and their FT's. Overall, in the final fit, five variables relating to three components were allowed to vary: three bond distances (one in δ-Pu and two in α'-Pu), and the Debye-Waller factors for the main δ-Pu component and for the short bond component of the α'-Pu. Fixing S_0^2 and ΔE_0 and using a consistent k-range avoid correlation problems between S_0^2 and the Debye-Waller factors σ^2, as well as between

ΔE_0 and the distances R. Fixing these parameters and the k-range ensures a meaningful comparison of values for the distances and Debye-Waller factors at different temperatures in the following thermal Debye analysis.

C. EXAFS modeling of δ'-Pu phase

The δ' metastable phase of Pu/Ga alloys consists of Ga dopant atoms trapped in an δ-Pu matrix. The δ-Pu structure is unusual for a pure metal in that the nearest-neighbor distances form a distribution of values rather than one well-defined value. This distribution varies for each of the eight unique crystallographic sites (Pu1 through Pu8). The distribution of bond lengths in each site is split between four (on average) shorter bonds of lengths 2.57-2.78 Å and ten (on average) longer bonds of lengths 3.19-3.71 Å.[19] Including all of these bond lengths in a fit to the EXAFS data would not be meaningful, so we chose to approximate the bond length distribution in δ'-Pu by two component peaks in the EXAFS FT, which correspond to the average short and long nearest-neighbor bond lengths, $R_{\delta 1}$ and $R_{\delta 2}$, respectively.

The eight δ'-Pu site structures (with either Pu or Ga as the central atom) were simulated using FEFF8.1[16, 17] to give eight different EXAFS patterns, as shown in Figure 2. The effect of temperature was included using the DEBYE card of FEFF8.1 and a pure δ-Pu Debye temperature, Θ_D, of 201 K.[20] The EXAFS spectra for all eight sites were averaged with equal weights to produce the spectrum seen at the tops of Figures 2(a) and 2(b). The FT of the averaged model EXAFS (top, Figure 2(b)) has two main peaks corresponding to the short and long bond lengths described above.

As seen in Figure 2, there is quite a large variation in the model EXAFS spectra

and in particular the model EXAFS FT's for each of the Pu sites. Therefore, the site-averaged EXAFS are expected to have considerable static disorder in the short and long bond length distributions. In addition, detailed examination of the Ga EXAFS for δ'-Pu should determine if random substitution of Ga in each of the eight Pu sites in δ'-Pu is a valid assumption, or if there is preferential population of one or several of the sites.

In order to determine appropriate starting parameters, i.e. coordination number N, distance R, and Debye-Waller factor σ^2 for these two δ' shells, the site-averaged model δ'-Pu EXAFS data was fit as a function of temperature using a two-shell fit. The k range and S_0^2 were fixed to match that of the experimental data, and the coordination numbers were fixed at $N_{\delta 1} = 4$ and $N_{\delta 2} = 10$ in agreement with the site-averaged coordination numbers of δ-Pu. For each temperature, the ratio of the fit Debye-Waller factors for the two shells was determined. The Debye-Waller factor ratio was found to be almost constant over the entire temperature range, with values of $\sigma_{\delta 2}^2 / \sigma_{\delta 1}^2 = 1.64$ and 1.60 for the Pu and Ga EXAFS, respectively. This ratio was then used to link the Debye-Waller factors of the $R_{\delta 1}$ and $R_{\delta 2}$ shells for the δ'-Pu part of the fit to the measured EXAFS of the mixed phase alloy.

III. RESULTS

A. EXAFS data and structural results

Figure 3 compares the Pu L_{III} EXAFS FT's of the partially transformed (70% δ-Pu / 30% δ'-Pu) 1.9 at% Ga-doped Pu sample to that of the untransformed (100% δ-Pu) 1.9

at% Ga-doped Pu sample, measured at T = 150 K. The FT represents a pseudoradial distribution function, and its peaks are shifted to lower R values compared with real atom-to-atom distances. This a result of the phase shift, δ, associated with the absorber-scatterer interactions. The height of the main peak at R+δ ~ 3.0 Å is seen to decrease by ~30% for the partially transformed alloy relative to the 100% δ-Pu alloy, while the peak at R+δ ~ 2.5 Å increases slightly for the partially transformed alloy. The different behavior of these two peaks upon transformation suggests that more than one component is required for the fit, as expected for a mixed phase sample. The EXAFS data for the untransformed sample is fit well by a single nearest neighbor peak at R_δ = 3.28 Å and a coordination number of N_δ = 12 (100% δ-Pu), in agreement with the fcc δ-Pu structure. The main peak of the partially transformed alloy is fit well with a similar δ-Pu component, with the coordination number reduced to N_δ = 8.4 (70% δ-Pu). However, the peak in Figure 3(b) at R+δ ~ 2.5 Å is not fit well with the single δ-Pu component, since the low-R shoulder of the δ-Pu component does not have enough intensity at this shorter distance. The peak at R+δ ~ 2.5 Å is unique to the partially transformed sample. Since the fit is improved by adding a δ'-Pu short bond component at $R_{\delta 1}$ = 2.62 Å, this peak can be attributed to the short bonds in δ'-Pu, which range from 2.57-2.78 Å in length.[19] The coordination number for this component is $N_{\delta 1}$ = 1.2, which is 30% of the average δ'-Pu short bond coordination number of 4. In order to correctly model the Pu local environment in δ'-Pu, a longer bond component with $R_{\delta 2}$ = 3.36 Å is included with $N_{\delta 2}$ = 3.0, which is 30% of the average δ'-Pu long bond coordination number of 10. Figure 3(c) depicts the three components used in the fit to the mixed phase alloy. With the addition of the two δ'-Pu components, the reduced σ^2 value decreases by more than a

factor of six compared to that for a single-component, 100% δ-Pu fit. Thus with EXAFS we have identified the signatures of both the δ and δ' local environments of Pu within this mixed phase alloy.

A comparison of the Ga K EXAFS for the untransformed and partially transformed samples is given in Figure 4. Similar to the case of the Pu EXAFS, the main peak at R+Δ ~3.1 Å is seen to decrease by ~30% for the partially transformed alloy relative to the 100% δ-Pu alloy, and the peak at R+Δ ~ 2.6 Å decreases slightly for the partially transformed alloy. A single-component 100% δ-Pu fit underestimates the peak at R+Δ ~ 2.6 Å, and the fit of the Ga EXAFS for the mixed phase sample is improved by including the two δ'-Pu components. This indicates that the Ga atoms are present in both the δ-Pu and δ'-Pu phase within the sample. The coordination numbers were fixed to the same values for both Pu and Ga EXAFS, i.e. N_{δ} = 8.4, $N_{\delta 1}$ = 1.2, and $N_{\delta 2}$ = 3.0, which assumes that the Ga did not migrate substantially from one phase to the other upon or after transformation.[2] For the Ga K EXAFS case, the reduced σ^2 value of the three-component fit to the data is 35% less than the corresponding value for the single-component 100% δ-Pu fit.

The first effect revealed by these data is the overall contraction of Pu atoms around the Ga sites in δ-Pu, R_{δ}(Ga-Pu) = 3.17 Å, relative to the environment around the Pu sites, R_{δ}(Pu-Pu) = 3.28 Å. This contraction of about 4% (ΔR_{δ} = –0.11 Å) is comparable to that observed by earlier EXAFS studies on δ-Pu.[11, 21-23]

Secondly, both the Pu and Ga EXAFS demonstrate mixed phase character and show the existence of short and long bond components whose lengths agree with the expected average structure of δ'-Pu. In addition, by comparison of the measured δ'-Pu

component bond lengths to the model EXAFS calculations shown in Figure 2, the Ga in δ'-Pu best matches the site-averaged spectra. This indicates that Ga atoms are randomly substituting for Pu atoms in the δ'-Pu portion of this mixed phase sample.

Thirdly, the short and long bond lengths for the δ'-Pu component are contracted for the Ga-Pu bonds with respect to the Pu-Pu bonds, although less than in the case of δ-Pu: $\Delta R_{\delta 1} = -0.03$ Å and $\Delta R_{\delta 2} = -0.06$ Å. The smaller contraction around the Ga site in δ'-Pu relative to that in δ-Pu may relate to the solubility of Ga atoms in the respective phases. This hypothesis can be further tested by measuring the temperature dependence of the EXAFS Debye-Waller factors, in order to determine the relative strength of the Ga-Pu and Pu-Pu bonds in each of the phases.

B. Vibrational analysis

Figures 5(a) and 5(b) show the k^3-weighted Pu EXAFS L_{III} data and the corresponding FT's for the 70% δ-Pu / 30% δ'-Pu sample as a function of temperature. As the sample is cooled from 293 to 13 K, the EXAFS amplitude increases systematically due to decreased thermal motion of the atoms in the lattice. This effect is equally visible in the corresponding FT's. As the temperature is lowered, the intensities of the FT peaks increase dramatically, and higher R peaks appear, corresponding to neighboring atoms in more distant shells. These peaks are consistent with those expected for the δ-Pu fcc lattice. No peaks are readily discerned in the FT at high R for the outer shells of the δ'-Pu lattice, due to the distortions in the δ'-Pu phase. The first shell Pu-Pu peak seen at R+Δ ~ 3.0 Å corresponds to 12 Pu near neighbors in the δ-Pu fcc structure. The second and third shell peaks at ~4.3 and 5.4 Å which correspond to real interactions at 4.64 and 5.68

Å are clearly affected by thermal effects and become distinguishable only for T ≤ 80 K. These results for the δ-Pu components of the EXAFS are similar to our previous Pu L_{III} EXAFS thermal series taken on a 3.3 at% Ga-doped δ-Pu sample.[11]

The most dramatic effect depicted in this data set is the difference in the temperature dependence between the Pu-Pu Debye-Waller factors σ^2 for the δ-Pu and δ'-Pu components of the fits. This is demonstrated in Figure 5(b) by the changes in the relative sizes of the peaks at R+Δ ≈ 3.0 Å (mostly δ-Pu in character) and at R+Δ ≈ 2.4 Å (mostly δ'-Pu in character) as the temperature is increased. At low temperatures, the δ-Pu peak dominates the EXAFS FT, but this peak broadens and decreases in height more rapidly than the δ'-Pu peak, such that at room temperature the two peaks are of almost equal intensity.

The Ga K-edge raw k^3-weighted EXAFS and corresponding FT's are shown in Figs. 6(a) and 6(b). The spectra are dominated by the peak at R+Δ ~3.1 Å, attributed to the first shell Ga-Pu interactions within the δ-Pu part of the sample. At lower temperatures (T < 50 K), the FT's reveal second and third shell Ga-Pu interactions in δ-Pu near 4.4 and 5.4 Å. Unlike the Pu L_{III} EXAFS FT's, the ratio of the relative intensities of the peaks at R+Δ ≈ 3.1 Å (mostly δ-Pu in character) and at R+Δ ≈ 2.6 Å (mostly δ'-Pu in character) is almost unchanged as the temperature is increased. This indicates a similar temperature dependence of the Ga-Pu bond vibrational amplitude in both δ'-Pu and δ-Pu phases.

The curve-fitting results summarized in Tables I and II serve to quantify the different temperature dependent and static structural effects for the Pu and Ga sites in this mixed phase material. At each temperature, the Pu and Ga EXAFS data were fit with a

single δ-Pu component and two δ'-Pu components, with the same fixed parameters, constraints, and fit variables (R_{δ}, $R_{\delta 1}$, $R_{\delta 2}$, σ_{δ}^2, and $\sigma_{\delta 1}^2$) as the fits in Figures 3 and 4.

The values of the bond lengths R_{δ}, $R_{\delta 1}$, and $R_{\delta 2}$ do not change dramatically with temperature. In addition, the fixed coordination numbers corresponding to a 70% δ-Pu / 30% δ'-Pu phase composition produce high-quality fits with systematically increasing Debye-Waller factors over the entire temperature range, indicating that the relative fractions of the δ'-Pu and δ-Pu phases do not change significantly as the temperature is changed. This is consistent with the δ-Pu –> δ'-Pu transformation being essentially complete for this alloy over the time scale of the pre-experimental treatment.[2-3] In addition, the relative Ga population in the two phases does not change with temperature. The Pu and Ga EXAFS were measured again in a later experiment, after the sample sat at room temperature for eight months. Upon comparing the results of the two experiments (22 days versus 9 months after the initial δ –> δ' transformation), no significant change was observed in the relative intensities of δ'-Pu and δ-Pu components in the EXAFS from either element. This observation confirms that under ambient conditions, the diffusion rate of Ga "trapped" in δ'-Pu is very slow.[2]

The values of σ^2 for the δ'-Pu and δ-Pu EXAFS components increase with temperature consistent with greater thermal disorder, as expected. However, according to Table I, the Pu-Pu first shell for δ-Pu shows much greater disorder at higher temperatures than the corresponding Pu-Pu shell in δ'-Pu. In contrast, at low temperatures, the Debye-Waller factor for δ'-Pu is larger than for δ-Pu. This can be understood from the lower symmetry of the δ'-Pu structure relative to well-ordered fcc δ-Pu, since at the lowest temperatures, the main contribution to the Debye-Waller factor is from static (structural)

disorder and not thermal disorder. The crossover temperature at which the Debye-Waller factors for the δ and δ' components are equal is near T $\approx$ 80K.

To study these thermal effects more carefully, the temperature dependence of the EXAFS Debye-Waller factors is modeled by employing the correlated-Debye model to determine the Debye temperature. This formalism[24-25] previously has been used to determine the pair-specific Debye temperatures for Pu-Pu and Ga-Pu bonds in 3.3 at% Ga-doped single-phase δ-Pu.[11] For the mixed phase sample, we use EXAFS to separate the differing thermal dependencies of the nearest neighbor interactions in δ'-Pu and δ-Pu. Using this formalism, we obtain the fits shown in Figure 7. The fit of the model to the data is very good for both phases, indicating that the local pair vibrations can be described using the correlated-Debye model. From these fits, we determine pair-specific correlated-Debye temperatures Θ_{cD} of 120 ± 3 K and 159 ± 13 K for the Pu-Pu first shells in δ-Pu and δ'-Pu, respectively (Table III). The value for δ-Pu is consistent with Debye temperatures for δ-Pu (105-132 K, Ref. 11) determined in other studies. The value of the Debye temperature for δ'-Pu, which has not been reported previous to this work, is similar to that of pure α-Pu (160-200 K, from Ref. 26). The T=0 intercept of the plot of σ^2 versus temperature equals $\sigma^2_{static} + \sigma^2_{ZPM}$, where σ^2_{ZPM} is the quantum zero-point motion of the atoms in the bond. From the correlated Debye fit, the static disorder Debye-Waller factors for Pu-Pu bonds in δ-Pu and δ'-Pu are σ^2_{static}(Pu-Pu in δ-Pu) = 0.0002 ± 0.0003 and σ^2_{static}(Pu-Pu in δ'-Pu) = 0.0021 ± 0.0006. The near-zero σ^2_{static} value for fcc δ-Pu and the large value for monoclinic δ'-Pu reflects the differing degrees of asymmetry in the local structure of these two unit cells.

The temperature dependence of the Debye-Waller factor of the Ga-Pu

components in δ'-Pu and δ-Pu was also analyzed. Here, the Debye temperatures Θ_{cD} are equal to 188 ± 12 K and 203 ± 15 K for the Ga-Pu first shells in δ-Pu and δ'-Pu, respectively (Table III). Within experimental error, the measured Debye temperatures for the Ga-Pu bond in both δ-Pu and δ'-Pu are equal to the previously reported value of 202.6 ± 3.7 K for a single-phase 3.3 at% Ga-doped δ-Pu alloy.[11] Unlike the case for the Pu-Pu bond, where the Debye temperatures and consequently the bond strengths are quite different for the δ'-Pu and δ-Pu phases, there is less disparity in the Ga-Pu bond Debye temperatures and bond strengths for the two phases.

IV. DISCUSSION

In δ-Pu, the Ga-Pu bond Debye temperature is much larger than that of the Pu-Pu bonds, which is consistent with previous observations on a 3.3 at% Ga-doped δ-Pu alloy.[11] In δ'-Pu, the Ga-Pu bond Debye temperature is also larger than the Pu-Pu bond Debye-temperature, but the difference is not as large as in δ-Pu. The Debye temperature Θ_{cD} may be directly related to the force constant f_E of the bond vibration through the relation[27-28]

$$f_E = \mu(0.787\Theta_D)^2 = 0.620\mu k_B^2\Theta_{cD}^2/\hbar^2 \quad , \qquad (1)$$

where the reduced mass μ is equal to 54.0 amu for the Ga-Pu bond and 120.0 amu for the Pu-Pu bond. The constant 0.787 arises from assuming the relationship between the Debye and Einstein frequencies for an fcc lattice,[28] which is an average of the high-temperature and low-temperature trends. Table IV compares the relative sizes of the

force constants for the Ga-Pu and Pu-Pu bonds in both δ'-Pu and δ-Pu environments, as well as the ratios of the force constants across types of bond and across Pu phases.

The most interesting comparison is the ratio of Ga-Pu to Pu-Pu force constants in the δ'-Pu and δ-Pu phases, as this provides information on the role of Ga in the degree of stability of both of these phases. For δ-Pu, the Ga-Pu bond is similar or marginally stronger than the Pu-Pu bond. Thus the Ga-Pu bond has a strengthening role in the formation and "stabilization" of the δ-Pu phase. This result was also seen in the EXAFS study of the 3.3 at% Ga-doped δ-Pu alloy;[11] however, in that case the Ga-Pu force constant was ~50% stronger than the Pu-Pu force constant. In the case of δ'-Pu, the Ga-Pu force constant is ~30% weaker than the Pu-Pu force constant. The weaker Ga-Pu bond strength suggests that Ga does not strengthen the surrounding δ-Pu structure, and agrees with the observation that the δ'-Pu phase is metastable and that the randomly substituted Ga sites may eventually diffuse out of δ'-Pu, or possibly order into lower energy sites within the δ'-Pu structure.[29] However, as seen from the lack of change in the data after eight months, the kinetics of this Ga diffusion is very slow under ambient conditions. Thus, from the thermal dependence and phase specificity of EXAFS, we can directly measure bond properties which may be related to the change in role of Ga atoms from a phase "stabilizer" in δ-Pu to an insoluble dopant “trapped” in δ'-Pu.

By comparing the force constants of the different bonds across the two phases, we can determine how these changes in stabilization arise. The Pu-Pu bond strength is 40% smaller in δ-Pu than in δ'-Pu. Since bonding that is more covalent and delocalized is in general stronger than more ionic and localized bonding, the measured difference in Pu-Pu bond strengths may be related to the localization of 5f electronic charge in δ-Pu as

compared to the more delocalized metallic character of 5f electrons in δ-Pu.[4, 5] In contrast, the Ga-Pu bond strength decreases only by 15% in going from δ'-Pu to δ-Pu. Given that the measured Pu-Pu bond strength changes dramatically in going from δ'-Pu to δ-Pu while the Ga-Pu bond strength does not, and that the changes in the Pu-Pu bond strength may be related to the localization/delocalization of Pu 5f electronic charge, these results may suggest that the solubility or insolubility of Ga in δ-Pu and δ'-Pu, as well as the difference in stability of the δ-Pu and δ'-Pu phases, is due to the localization or delocalization of charge in the Pu matrix, rather than changes in the Ga-Pu bonding. This assertion is supported by the observation that a number of other elements – e.g. Al, In, Sc, and Ce – can be interchanged for Ga with the same effect of stabilizing the δ-Pu phase over a broader temperature range.[30]

V. CONCLUSION

Ga-Pu and Pu-Pu bond distances and vibrational amplitudes in both the δ' and δ phases of a partially transformed (70% δ-Pu / 30% δ'-Pu) 1.9 at% Ga-doped Pu alloy were determined as a function of temperature from the thermal behavior of the Pu L_{III}- and Ga K-edge EXAFS. Ga-Pu bonds are contracted 0.11 Å with respect to Pu-Pu bonds in the δ-Pu portion of the sample, while in δ'-Pu the Ga-Pu bond contraction with respect to the Pu-Pu bonds is smaller in magnitude (0.03 Å). The similarity of the Pu L_{III}- and Ga K-edge EXAFS in each phase indicates that Ga is substitutional for Pu in both δ-Pu and δ'-Pu. A comparison of the Ga EXAFS data with modeled EXAFS data of Ga in δ'-Pu indicates that Ga atoms are substituting randomly for Pu atoms in the δ'-Pu phase. The

lack of change in the Ga EXAFS components after eight months indicates the diffusion of the Ga from δ'-Pu to δ-Pu at ambient temperatures is very slow. Due to the large difference in nearest neighbor bond lengths in the two phases, the thermal behavior of the δ' and δ components may be resolved by EXAFS. From the temperature dependence of the EXAFS components for the phases, a large difference in the Pu-Pu bond Debye temperature is observed for the δ' and δ phases: $\Theta_D(\delta')$ = 159 ± 13 K versus $\Theta_D(\delta)$ = 120 ± 3 K. To our knowledge, this is the first measurement of the Debye temperature for δ'-Pu. The corresponding analysis for the Ga K EXAFS determines a Ga-Pu bond Debye temperature of $\Theta_D(\delta)$ = 188 ± 12 K in the δ-Pu phase, and $\Theta_D(\delta')$ = 203 ± 15 K in the δ'-Pu phase. The Pu Debye temperatures determined by EXAFS for Ga-containing δ'-Pu and δ-Pu are consistent with those from earlier studies on δ-Pu and δ-Pu phases determined using other methods.[11, 20, 26] The difference in Ga-Pu and Pu-Pu Debye temperatures in δ-Pu is consistent with our earlier result for a 3.3 at% Ga-doped δ-Pu alloy.[11] The difference in Pu-Pu Debye temperatures for the two phases may be related to the change from localized (δ) to delocalized (δ') 5f electrons in Pu.[4, 5] The intermediate strength of the Ga-Pu bond relative to the Pu-Pu bond in the two phases is consistent with Ga "stabilization" of the δ-Pu phase and Ga insolubility in the δ'-Pu phase. It would be interesting to use EXAFS to examine the nature of bonding of other "δ-stabilizing" dopant atoms – e.g. Al, In, Sc, and Ce – in the δ'-Pu / δ-Pu system.

ACKNOWLEDGEMENTS

This work (UCRL-JC-151541) was performed under the auspices of the U.S. Department

of Energy by University of California Lawrence Livermore National Laboratory under contract No. W-7405-Eng-48, under LDRD funding. Portions of this research were carried out at the Stanford Synchrotron Radiation Laboratory, a national user facility operated by Stanford University on behalf of the U.S. Department of Energy, Office of Basic Energy Sciences. This work was partially supported (C. H. B.) by the Office of Basic Energy Sciences, Chemical Sciences Division of the U. S. DOE, Contract No. DE-AC03-76SF00098.

REFERENCES

*Electronic address: nelson87@llnl.gov

[1]W. N. Miner and F. W. Schonfeld, in Plutonium Handbook, edited by O. J. Wick (The American Nuclear Society, La Grange Park, IL, 1990), p. 33.

[2]L. F. Timofeeva, in Aging Studies and Lifetime Extension of Materials, edited by L. G. Mallinson (Kluwer Academic / Plenum Publishers, 2001), p. 191. Timofeeva has shown that in true equilibrium below 100ºC, a mixture of δ-Pu and δ'-Pu will undergo eutectoid decomposition into Pu_3Ga and Ga-free α-Pu. At room temperature the kinetics of this reaction are exceedingly slow, such that for all practical purposes, the δ-Pu phase remains metastable for very long times (estimated at ~10^4 years).

[3]J. T. Orme, M. E. Faiers, and B. J. Ward, in Plutonium and Other Actinides, edited by H. Blank and R. Lindner (North-Holland Publishing Company, Amsterdam, 1976), p. 761.

[4]J. L. Smith and E. A. Kmetko, J. Less-Common Metals **90**, 83 (1983).

[5]J. M. Willis and O. Eriksson, Phys. Rev. B **45**, 13879 (1992).

[6]P. H. Adler, G. B. Olson, M. F. Stevens, and G. F. Gallegos, Acta Metall. Mater. **40**, 1073 (1992).

[7]T. G. Zocco, M. F. Stevens, P. H. Adler, R. I. Sheldon, and G. B. Olson, Acta Metall. Mater. **38**, 2275 (1990)

[8]J. R. K. Gschneidener, R. O. Elliott, and V. O. Struebing, in Plutonium 1960 (Cleaver-Hume, London, 1961), p. 99.

[9]P. H. Adler, Metall. Trans. A **22**, 2237 (1991).

[10]P. Weinberger, A. M. Boring, and J. Smith, Phys. Rev. B **31**, 1964 (1985).

[11]P. G. Allen, A. L. Henderson, E. R. Sylwester, P. E. A. Turchi, T. H. Shen, G. F. Gallegos, and C. H. Booth, Phys. Rev. B **65**, 214107 (2002).

[12]J. J. Bucher, P. G. Allen, N. M. Edelstein, D. K. Shuh, N. W. Madden, C. Cork, P. Luke, D. Pehl, and D. Malone, SRI Conf. Proc., Rev. Sci. Instrum. **67**, 3361 (1996).

[13]T. M. Hayes and J. B. Boyce, in Solid State Physics, edited by H. Ehrenreich, F. Seitz, and D. Turnbull (Academic, New York, (1982)), Vol. 37, p. 173.

[14]G. G. Li, F. Bridges, and C. H. Booth, Phys. Rev. B **52**, 6332 (1995).

[15]M. Newville, P. Livins, Y. Yacoby, J. J. Rehr, and E. A. Stern, Phys. Rev. B **47**, 14126 (1993).

[16]J. J. Rehr, J. Mustre de Leon, S. I. Zabinsky, and R. C. Albers, Phys. Rev. B **44**, 4146 (1991).

[17]J. J. Rehr, J. Mustre de Leon, S. I. Zabinsky, and R. C. Albers, J. Am. Chem. Soc. **113**, 5135 (1991).

[18]F. H. Ellinger, J. Met. **8**, 1256 (1956).

[19]W. H. Zachariasen and F. H. Ellinger, Acta. Cryst. **16**, 777 (1963).

[20]A. C. Lawson, J. A. Goldstone, B. Cort, R. I. Sheldon, and E. M. Foltyn, J. Alloys and Compounds **213/214**, 426 (1994).

[21]L. E. Cox, R. Martinez, J. H. Nickel, S. D. Conradson, and P. G. Allen, Phys. Rev. B **51**, 751 (1995).

[22]P. Faure, B. Deslandes, D. Bazin, C. Tailland, R. Doukhan, J. M. Fournier, and A. Falanga, J. Alloys Compd. **244**, 131 (1996).

[23]N. Richard, P. Faure, P. Rofidal, J. L. Truffier, and D. Bazin, J. Alloys Compd. **271-273**, 879 (1998).

[24]E. D. Crozier, J. J. Rehr, and R. Ingalls, in X-Ray Absorption: Principles, Applications, Techniques of EXAFS, SEXAFS, XANES, edited by D. Konigsberger and R. Prins (Wiley, New York, 1988), p. 373.

[25]G. B. Beni and P. M. Platzman, Phys. Rev. B **14**, 1514 (1976).

[26]J. A. Lee and M. B. Waldron, in Inorganic Chemistry, Series Two (Baltimore: University Park Press, 1975), Vol. 7, Chap. 7, p. 250.

[27]J. J. Rehr and R. C. Albers, Rev. Mod. Phys. **72**, 621 (2000).

[28]P. P. Lottici, Phys. Rev. B **35**, 1236 (1987).

[29]B. Sadigh and W. G. Wolfer, article submitted to Nature.

[30]P. Chiotti, V. V. Akhachinskij, I. Ansara, and M. H. Rand, The Chemical Thermodynamics of Actinide Elements and Compounds (The American Nuclear Society, International Atomic Energy Agency, Vienna, 1981), Vol. 5, p. 231.

Table I. Pu L_{III}-edge EXAFS fitting results. EXAFS data were fitted over the k-range [2.8, 12.5 $Å^{-1}$] by three components, one for the δ-Pu phase nearest neighbor shell and the other two for the short and long nearest neighbor bonds in δ'-Pu. The fractional populations of the two phases are 70% δ-Pu and 30% δ'-Pu by mass, as deduced from optical microscopy. The coordination numbers were scaled by the fractional populations and fixed at N_{δ} = 8.4 (70% of 12), $N_{\delta 1}$ = 1.2 (30% of 4), and $N_{\delta 2}$ = 3.0 (30% of 10). S_0^2 and ΔE_0 were fixed at 0.55 and –20.0 eV, respectively, and the ratio of the Debye-Waller factors for the short and long δ'-Pu components was fixed at $\sigma_{\delta 2}^2 / \sigma_{\delta 1}^2 = 1.64$ as determined by two-component fits to δ'-Pu EXAFS simulated using FEFF.

	□-Pu shell [a]		First □'-Pu shell		Second □'-Pu shell	
Sample Temp(K)	Pu-Pu $R_{□}$ (Å)	Pu-Pu $□_{□}^2$ (Å^2)	Pu-Pu $R_{□1}$ (Å)	Pu-Pu $□_{□1}^2$ (Å^2)	Pu-Pu $R_{□2}$ (Å)	Pu-Pu $□_{□2}^2$ (Å^2)
13	3.276	0.00236	2.628	0.00328	3.411	0.00535
30	3.280	0.00295	2.633	0.00374	3.435	0.00598
50	3.281	0.00331	2.623	0.00399	3.457	0.00652
80	3.276	0.00441	2.632	0.00447	3.426	0.00732
110	3.275	0.00596	2.624	0.00451	3.414	0.00739
150	3.276	0.00792	2.627	0.00554	3.423	0.00906
175	3.276	0.00986	2.626	0.00767	3.419	0.01256
200	3.272	0.01083	2.629	0.00700	3.418	0.01145
293	3.267	0.01510	2.634	0.00934	3.418	0.01528

[a] Errors in R and $□^2$ are estimated to be ± 0.005 Å and ± 10% based on EXAFS fits to model compounds, cf. Ref. 14.

Table II. Ga K-edge EXAFS fitting results. EXAFS data were fitted over the k-range [2.6, 12.4 Å^{-1}] by three components, one for the δ-Pu phase nearest neighbor shell and the other two for the short and long nearest neighbor bonds in δ'-Pu. The fractional populations of the two phases are 70% δ-Pu and 30% δ'-Pu by mass, as deduced from optical microscopy. The coordination numbers were scaled by the fractional populations and fixed at N_{δ} = 8.4 (70% of 12), $N_{\delta 1}$ = 1.2 (30% of 4), and $N_{\delta 2}$ = 3.0 (30% of 10). S_0^2 and ΔE_0 were fixed at 0.85 and +6.2 eV, respectively, and the ratio of the Debye-Waller factors for the short and long δ'-Pu components was fixed at $\sigma_{\delta 2}^2 / \sigma_{\delta 1}^2 = 1.60$ as determined by two-component fits to δ'-Pu EXAFS simulated using FEFF.

	δ-Pu shell [a]		First δ'-Pu shell		Second δ'-Pu shell	
Sample Temp(K)	Ga-Pu R_{δ} (Å)	Ga-Pu σ_{δ}^2 (Å^2)	Ga-Pu $R_{\delta 1}$ (Å)	Ga-Pu $\sigma_{\delta 1}^2$ (Å^2)	Ga-Pu $R_{\delta 2}$ (Å)	Ga-Pu $\sigma_{\delta 2}^2$ (Å^2)
13	3.174	0.00591	2.598	0.00591	3.354	0.00947
50	3.178	0.00469	2.589	0.00535	3.370	0.00858
80	3.178	0.00522	2.624	0.00497	3.346	0.00797
110	3.173	0.00803	2.598	0.00716	3.330	0.01148
150	3.176	0.00950	2.607	0.00901	3.342	0.01445
293	3.172	0.01660	2.608	0.01417	3.388	0.02274

[a] Errors in R and σ^2 are estimated to be ± 0.005 Å and ± 10% based on EXAFS fits to model compounds, cf. Ref. 14.

Table III. Debye temperatures Θ_D in Kelvin and static disorder Debye-Waller factors σ^2_{static} in Å^2 for the Ga-Pu and Pu-Pu bonds in both the δ'-Pu and δ-Pu phases as determined from the fits of the temperature dependence of the EXAFS component Debye-Waller factors to the correlated Debye model.

	Pu-Pu bond		Ga-Pu bond	
Phase	Θ_D (K)	σ^2_{static} (Å^2)	Θ_D (K)	σ^2_{static} (Å^2)
δ-Pu	120 ± 3 K	0.0002 ± 0.0003 Å^2	188 ± 12 K	0.0015 ± 0.0009 Å^2
δ'-Pu	159 ± 13 K	0.0021 ± 0.0006 Å^2	203 ± 15 K	0.0023 ± 0.0008 Å^2

Table IV. Force constant f_E in dynes/cm for the Ga-Pu and Pu-Pu bonds in both the δ'-Pu and δ-Pu phases as determined from the fits of the temperature dependence of the EXAFS component Debye-Waller factors to the correlated Debye model.

	Force constant f_E (10^4 dynes/cm)		
Phase	Pu-Pu bond	Ga-Pu bond	$f_{Ga\text{-}Pu}$ / $f_{Pu\text{-}Pu}$ ratio
δ-Pu	3.07 ± 0.15	3.38 ± 0.43	1.10 ± 0.15
δ'-Pu	5.36 ± 0.88	3.91 ± 0.58	0.73 ± 0.16
f_{δ} / $f_{\delta'}$ ratio	0.57 ± 0.10	0.87 ± 0.17	

FIGURE CAPTIONS

Figure 1. Optical micrographs of the 1.9 at% Ga-doped Pu alloy, at two levels of magnification. (a) 100% δ-Pu alloy. (b) 75% δ-Pu / 25% α'-Pu by volume. The arrow in (b) points to an α'-Pu martensitic platelet.

Figure 2. (a) Modeled k^3-weighted Ga K-edge EXAFS and (b) corresponding Fourier transforms (FT's) over the k-range [3.0 $Å^{-1}$, 15.0 $Å^{-1}$] for Ga substituted in each of the eight Pu sites (Pu1-Pu8) in α'-Pu. EXAFS were modeled using scattering phases and amplitudes calculated from the program FEFF8.1 at a temperature of 170 K. The top spectra in (a) and (b) correspond to the site-averaged spectra.

Figure 3. Fourier transforms (FT's) of the Pu L_{III} EXAFS data for the (a) untransformed (100% δ-Pu) alloy and (b) partially transformed 70% δ-Pu / 30% α'-Pu alloy, along with the FT's of the fits to the data. (c) The three components of the fit in part (b). The EXAFS for the untransformed sample is fit well by a single δ-Pu component at R = 3.26 Å, while the partially transformed alloy has part of its spectral weight shifted to lower R values (R = 2.62 Å), and requires additional α'-Pu components for an accurate fit to the data.

Figure 4. FT's of the Ga K EXAFS data for the (a) untransformed (100% δ-Pu) alloy and (b) partially transformed 70% δ-Pu / 30% α'-Pu alloy, along with the FT's of the fits to the data. (c) The three components of the fit in part (b). The EXAFS for the

untransformed sample is fit well by a single δ-Pu component at R = 3.18 Å, while the partially transformed alloy has part of its spectral weight shifted to lower R values (R = 2.61 Å), and requires additional δ'-Pu components for an accurate fit to the data.

Figure 5. (a) Pu L_{III}-edge k^3-weighted transmission EXAFS data and (b) FT's of the EXAFS for the partially transformed 70% δ-Pu / 30% δ'-Pu alloy. For each plot, the solid line is the data, and the dashed line is the three-component fit to the data. FT's in (b) were taken over the k-ranges shown in (a). Note the change in relative FT peak heights of the δ and δ' components at R+Δ ~ 3.0 Å and 2.4 Å, respectively, throughout the temperature range.

Figure 6. (a) Ga K-edge k^3-weighted fluorescence EXAFS data and (b) FT's of the EXAFS for the partially transformed 70% δ-Pu / 30% δ'-Pu alloy. For each plot, the solid line is the data, and the dashed line is the three-component fit to the data. FT's in (b) were taken over the k-ranges shown in (a). Note the similarity of the relative FT peak heights of the δ and δ' components at R+Δ ~ 3.1 Å and 2.6 Å, respectively, throughout the temperature range.

Figure 7. Plot of Debye-Waller factor vs. temperature for first shell Pu-Pu bonds in δ'-Pu and δ-Pu as determined from fits to the Pu L_{III}-edge EXAFS. The data are plotted along with fits generated using the correlated Debye model.

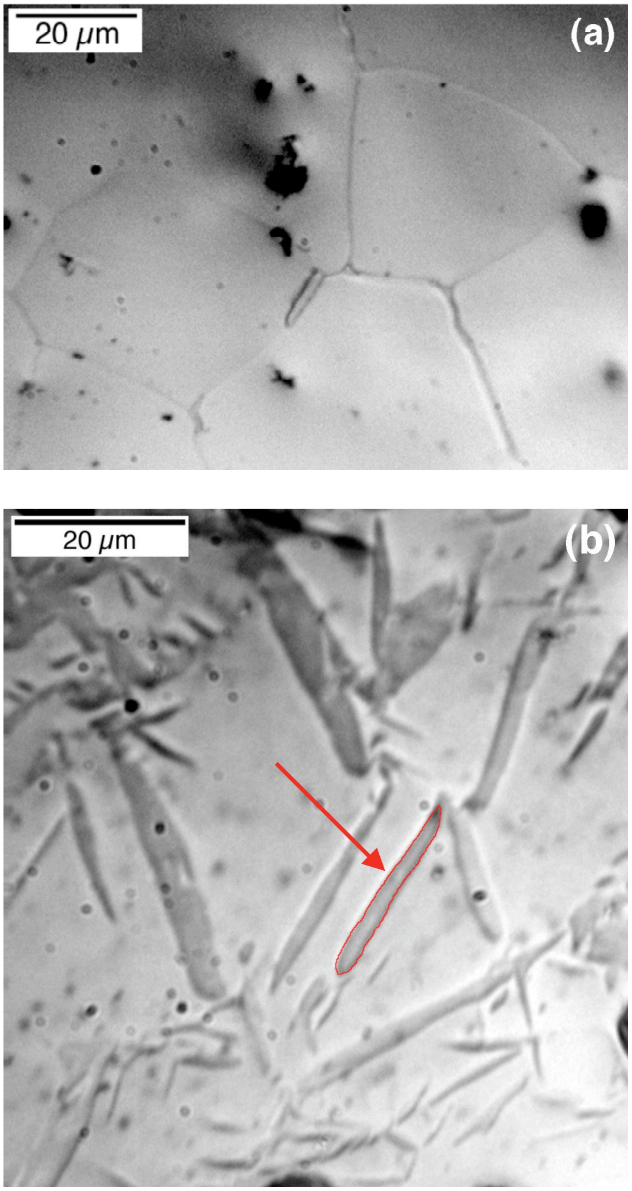

Figure 1.

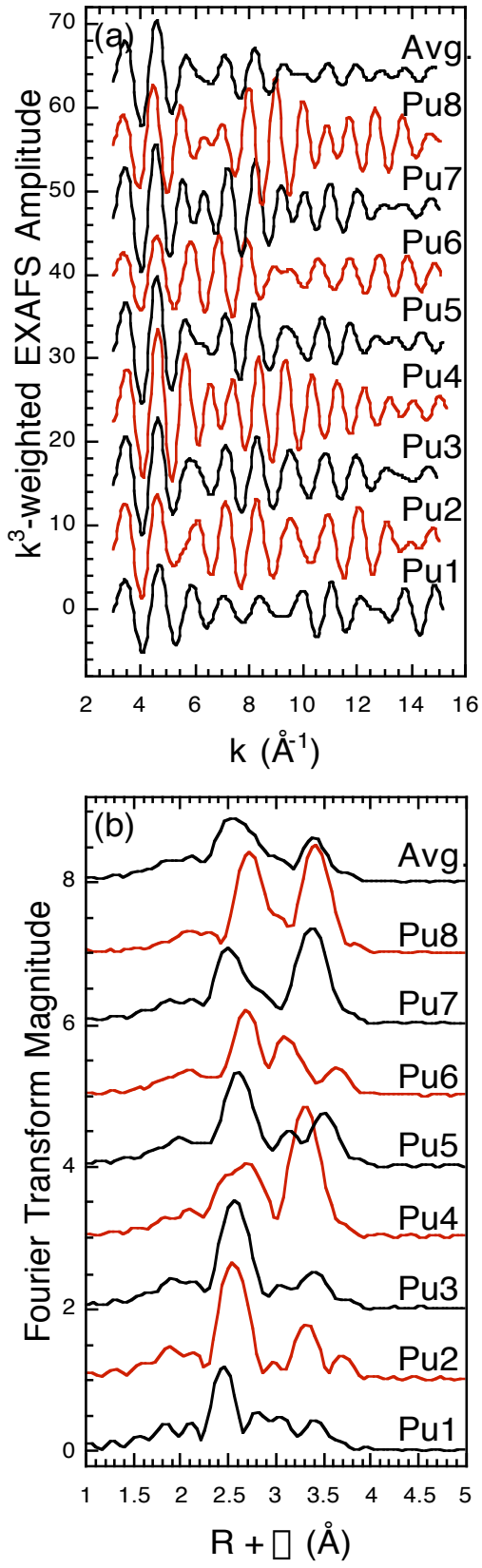
(a)
Avg.
Pu8
Pu7
Pu6
Pu5
Pu4
Pu3
Pu2
Pu1
k³-weighted EXAFS Amplitude
k (Å⁻¹)
(b)
Avg.
Pu8
Pu7
Pu6
Pu5
Pu4
Pu3
Pu2
Pu1
Fourier Transform Magnitude
R + □ (Å)

Figure 2.

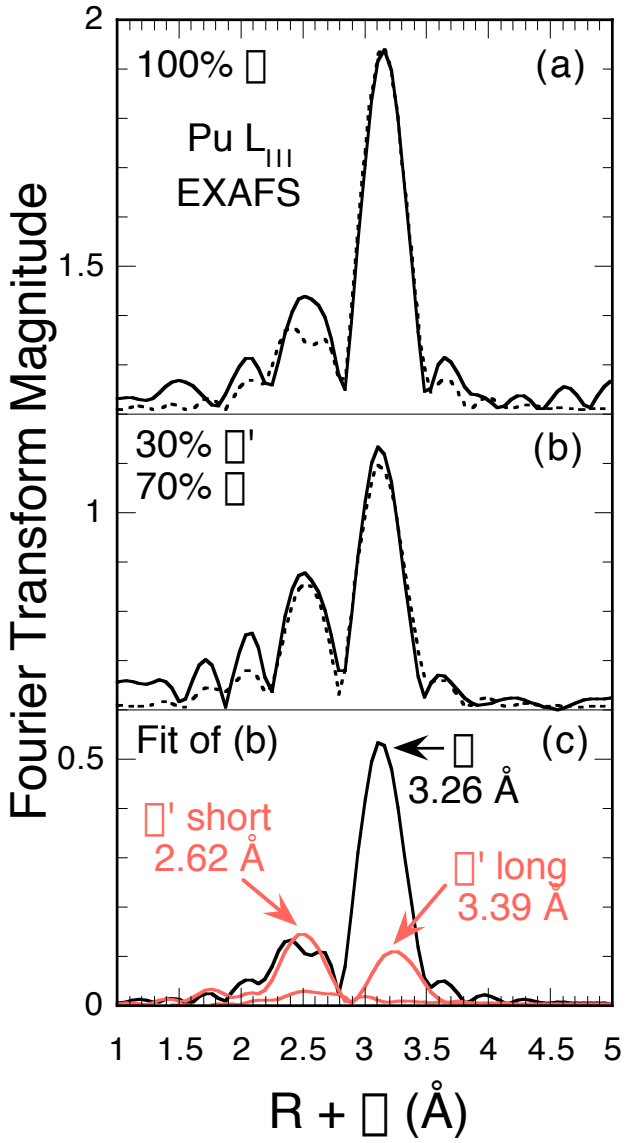
Fourier Transform Magnitude
R + Δ (Å)
100% δ
(a)
Pu L$_{III}$
EXAFS
30% δ'
70% δ
(b)
Fit of (b)
(c)
δ
3.26 Å
δ' short
2.62 Å
δ' long
3.39 Å
0
0.5
1
1.5
2
1
1.5
2
2.5
3
3.5
4
4.5
5

Figure 3.

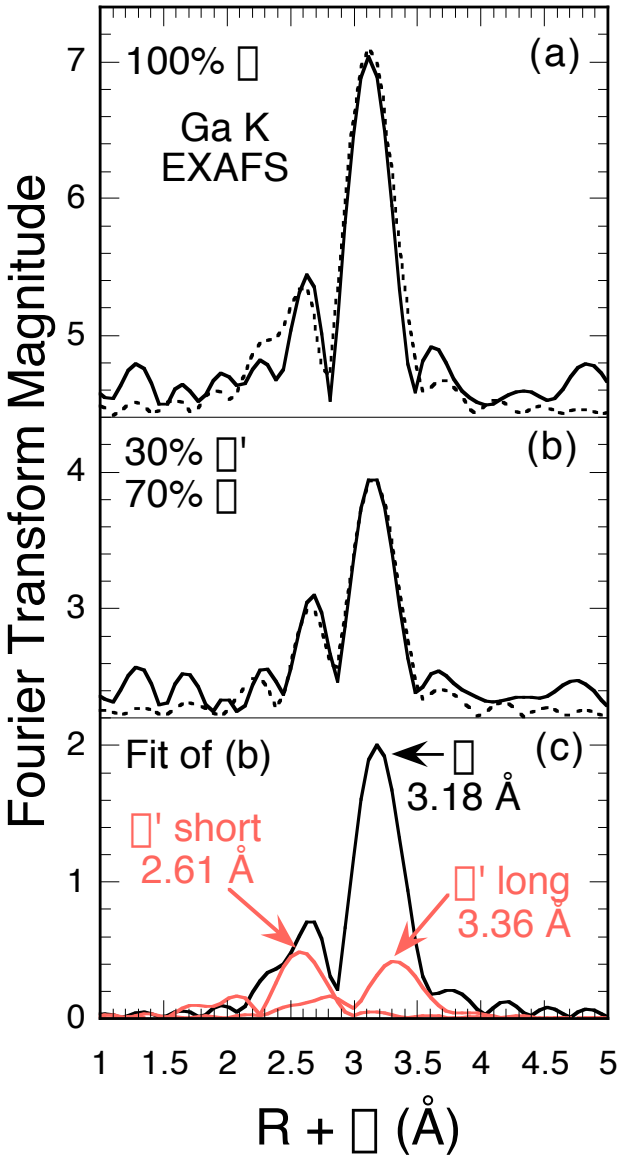
100% □
(a)
Ga K
EXAFS
30% □'
70% □
(b)
Fit of (b)
□
3.18 Å
(c)
□' short
2.61 Å
□' long
3.36 Å
Fourier Transform Magnitude
R + □ (Å)
0
1
2
3
4
5
6
7
1
1.5
2
2.5
3
3.5
4
4.5
5

Figure 4.

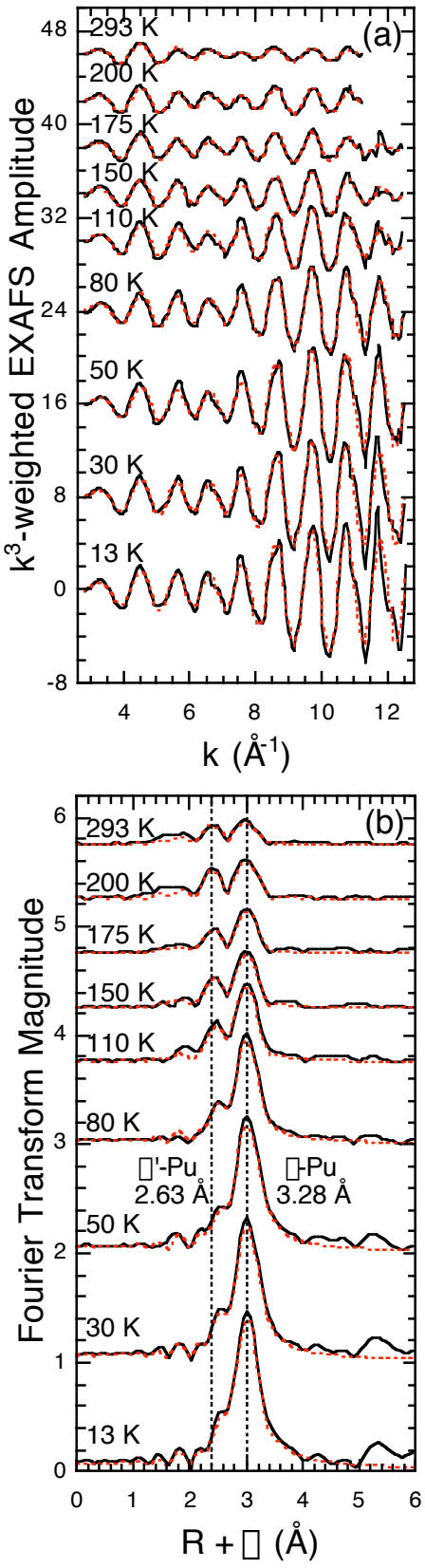
(a)
293 K
200 K
175 K
150 K
110 K
80 K
50 K
30 K
13 K
k³-weighted EXAFS Amplitude
k (Å⁻¹)
(b)
293 K
200 K
175 K
150 K
110 K
80 K
δ'-Pu
2.63 Å
δ-Pu
3.28 Å
50 K
30 K
13 K
Fourier Transform Magnitude
R + Δ (Å)

Figure 5.

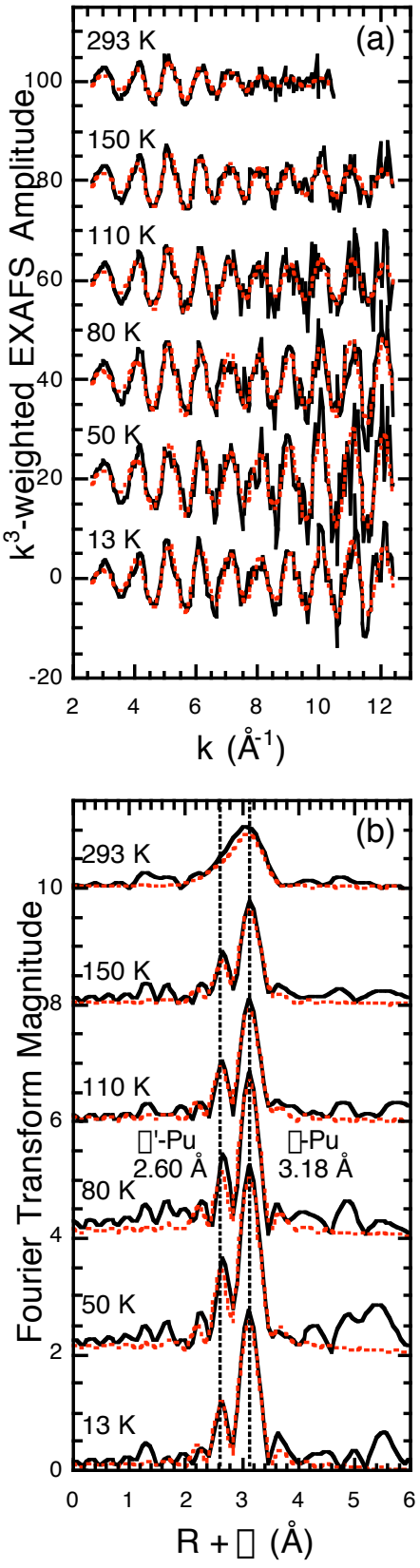
293 K
(a)
150 K
110 K
80 K
50 K
13 K
k³-weighted EXAFS Amplitude
k (Å⁻¹)
(b)
Fourier Transform Magnitude
δ'-Pu
2.60 Å
δ-Pu
3.18 Å
R + Δ (Å)

Figure 6.

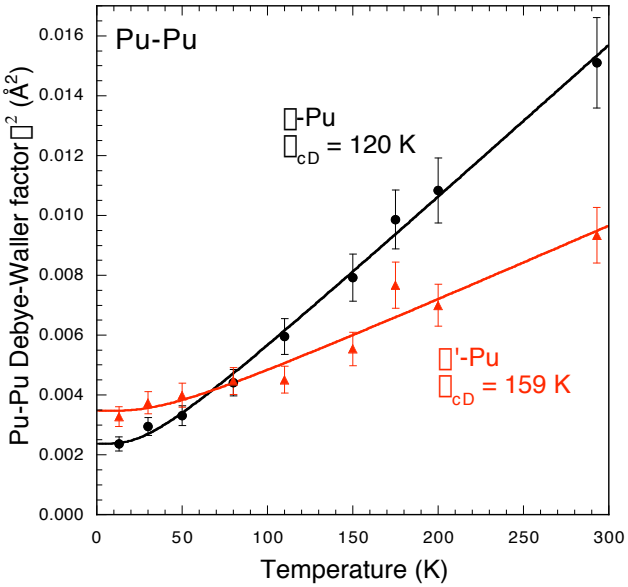
Pu-Pu
-Pu
cD = 120 K
'-Pu
cD = 159 K
Pu-Pu Debye-Waller factor 2 (Å2)
Temperature (K)
0.000
0.002
0.004
0.006
0.008
0.010
0.012
0.014
0.016
0
50
100
150
200
250
300

Figure 7.